CDF note 8104

First direct limit on the top quark lifetime

The CDF Collaboration
URL http://www-cdf.fnal.gov
(Dated: February 22, 2006)

We present the first direct limit on the top quark lifetime, measured in $t\bar{t}$ lepton+jets events using the lepton track impact parameter. The impact parameter distribution for selected events is fit to a probability distribution function which incorporates top events and expected backgrounds, and depends on the top quark lifetime. The measured lifetime is consistent with zero, conforming to the standard model expectation. We set an upper limit $c\tau_t < 52.5$ μm at 95% C.L.

Preliminary Results for Winter 2006 Conferences

I. INTRODUCTION

Using $t\bar{t}$ candidate events reconstructed as a leptonically decaying $W^{\pm}$ and ≥ 3 jets in the CDF detector at the Fermilab Tevatron, we have established the first direct limit on the top quark lifetime. We measure the distance between the top pair production point and the position of the $t \to b(W \to \ell\nu)$ decay by the separation of the lepton (electron or muon) track and the average $p\bar{p}$ collision point.

The top quark lifetime is constrained by the consistency of the Standard Model to be less than 10^{-24} s in the absence of extra lepton generations, by the electroweak coupling of $W^{\pm}$ to quark pairs and the CKM matrix element limits ($0.9990 < V_{tb} < 0.9992$ at 90% confidence level [1]). In contrast, there is ample room for long-lived t in the experimental data. This direct measurement of the top quark lifetime in $t\bar{t}$ candidate events at the Tevatron helps to confirm the identity of these particles as standard model t quarks. This method measuring the distance between the initial $p\bar{p}$ scattering and the $W^{\pm}$ decay vertex is also sensitive to unexpected production channels for t quarks by long-lived particles.

II. DATA SAMPLE AND EVENT SELECTION

For this measurement we use data collected with the CDF II detector between March 2002 and September 2004, corresponding to an integrated luminosity of 318 pb^{-1}. The CDF detector is described in detail elsewhere [2]. Events are first collected with an inclusive lepton trigger, requiring an electron with E_T >18 GeV or a muon with P_T >18 GeV/c.

From the lepton dataset we select an enriched sample of $t\bar{t}$ events. We accept collisions producing three or more jets with E_T >15 GeV, missing transverse energy in excess of 20 GeV, and either an isolated electron with $E_T > 20$ GeV or an isolated muon with $P_T > 20$ GeV/c. The selected electrons are additionally required to pass a photon conversion filter, which rejects track pairs consistent with a photon conversion to e^+e^- in the detector material. Events with multiple leptons passing the selection requirements are rejected, as are events consistent with Z^0 decays, in which the lepton forms an invariant mass between 76 and 106 GeV/c^2 with a loose lepton candidate.

To enhance the $t\bar{t}$ purity of these events we also require that one or more of the jets is identified (tagged) as a b-jet using a displaced vertex finding algorithm to detect the decay of long-lived b hadrons within the jet. To increase the precision of the lifetime measurement, the lepton track must be fit with at least three $r-\phi$ position measurements in the CDF silicon tracking system.

After this filtering of the data, we obtain 97 electron tracks and 60 muon tracks with which to measure the t lifetime.

III. MEASUREMENT OF THE TOP LIFETIME

Charged particles in CDF's 1.4 T magnetic field follow approximately helical trajectories with circular projections in the transverse $(x-y)$ plane. Our observable is the lepton impact parameter (d_0), which we define as the smallest distance between the transverse projection of the lepton track and the collision point. The collision point is measured as the beamline's (x, y) coordinates at the reconstructed z position of the collision.

We use the PYTHIA Monte Carlo program [3] and a detector simulation to determine the kinematics of standard model top quark decays which would be reconstructed and accepted by the event selection. These event kinematics are used to generate d_0 distributions of leptons from t decays, for lifetimes in the range 0 μm to 500 μm. From the kinematics of selected events we determine the impact parameter which would be measured with an ideal detector; the resolution of the CDF apparatus is determined directly from data.

We measure the impact parameter resolution of the CDF tracking system using a pure sample of prompt leptons from Drell-Yan events near the Z^0 resonance. Pairs of opposite-charge tight leptons of the same flavor, each satisfying the requirements for leptons in our signal sample, are selected if their invariant mass falls between 83 and 106 GeV/c^2. The background from non-Z^0 sources after these requirements is estimated to be less than 0.1%. The impact parameter distributions of these lepton tracks thus represent the intrinsic detector resolution, which in our calculation includes the uncertainty of the beam position (about 25 μm) as well as the error intrinsic to the single track helix measurement. The resolution functions, depicted in Figure 1, differ for electrons and muons because material interactions are more significant for electron tracks. These distributions are used to construct the observable impact parameter templates from the ideal distributions of the Monte Carlo.

The d_0 distributions from known backgrounds, described in Section IV, are added to the templates. The observed distributions of impact parameters for electrons and muons are then compared to the templates, and the value of $c\tau$ which maximizes the combined likelihood of our two datasets is selected as $c\tau_{\rm fit}$.

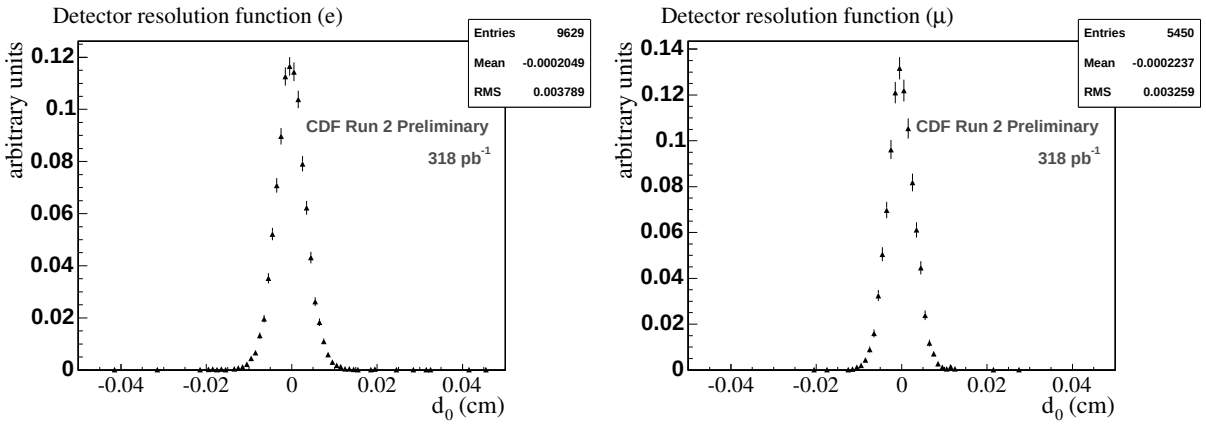

FIG. 1: Impact parameter resolution functions for electrons (left) and muons (right) with silicon tracks in the CDF detector.

IV. BACKGROUNDS

The dominant backgrounds in this analysis are "prompt," with no actual displacement between the interaction point and the lepton production position. The largest of these arise from direct production of a $W^{\pm}$ boson in association with several jets. Since a small fraction of the jets in these $W^{\pm}$+jets events are b- or c-jets, this background is largely suppressed by the requirement of a heavy flavor tag. Smaller prompt background contributions include Drell-Yan production of lepton pairs with additional jets, and diboson (WW,WZ, and ZZ) production.

The backgrounds which produce displaced electrons or muons and thereby mimic a long-lived top quark decay include $W^{\pm}$ and Z^0 production of leptonically decaying τ, semileptonic b and c quark decays producing an isolated lepton, and photon conversions which elude the conversion filter.

Electroweak production of single top quarks is considered a background only in constructing the Standard Model ($c\tau = 0\mu$m) template. If a long t lifetime were to be explained by a correspondingly small value of V_{tb}, even a lifetime of 1 μm would imply that the cross section for electroweak top production is suppressed by ten orders of magnitude.

A. Background multiplicity

Most of the backgrounds are estimated from their theoretical cross sections and an acceptance calculated by Monte Carlo simulation. These include the diboson backgrounds (WW, WZ, and ZZ), single top, and $Z^0 \to \tau^+\tau^-$. The simulated acceptance is also used for the $W^{\pm} \to \tau\nu$ and $Z^0 \to \ell^+\ell^-$+jets backgrounds, but in these cases the total number of events is normalized, using the theoretical cross section ratios, to the observed number of $W^{\pm} \to \ell\nu$+jets events. In this way we constrain the size of the $W^{\pm}/Z^0$+jets backgrounds to data, to reduce common acceptance systematics and theoretical uncertainties. The residual conversion background is estimated from the number of removed conversions and the inefficiency of the conversion filter.

After accounting for the aforementioned backgrounds and applying the constraints above, only the numbers of leptons from $W \to \ell\nu$+jets, $t\bar{t}$, and non-$W^{\pm}$ QCD sources are unknown. The last category includes fake leptons and those from semileptonic b and c decays, and is characterized by uncorrelated $\not\!\!E_T$ and lepton isolation. We separate these contributions using the different missing energy and isolation distributions and different b-tagging probabilities of the three processes.

Backgrounds in the electron and muon channels are summarized in Table I. The impact parameter distributions expected from these backgrounds are described below.

B. Background impact parameter distribution

The prompt backgrounds listed above are assumed to have the same impact parameter distribution as leptons in the Drell-Yan sample used to measure the detector resolution. However, the d_0 distributions of leptons from the non-$W^{\pm}$ QCD and τ decay backgrounds, and of electrons from photon conversions, must be modeled. The QCD background distribution is measured using isolated leptons in events with low missing energy, after removing the

	e events before tagging	tagged e events
all t	127.2± 16.2	78.4± 9.7
Prompt	266.7± 29.5	14.4± 3.6
Tau	17.8± 1.5	1.0± 0.4
QCD	19.8± 5.0	2.0± 0.9
Conversions	18.4± 1.6	1.2± 0.6

	μ events before tagging	tagged μ events
all t	79.8± 13.0	47.2± 7.7
Prompt	212.3± 24.0	10.5± 2.5
Tau	12.5± 1.2	0.7± 0.4
QCD	15.4± 3.9	1.6± 0.7

TABLE I: Signal and background estimates for the selected events in the electron (top) and muon (bottom) channels.

expected distribution from conversion electrons. It is consistent with the d_0 distribution of an admixture of promptly produced tracks and leptons from heavy flavor quark decays simulated with the HERWIG generator [4]. The conversion background d_0 distribution is also measured directly in a data sample of identified conversions. The τ backgrounds are simulated from Monte Carlo, using the measured detector resolution to correct the generated d_0 distribution. The sum of these contributions and the prompt background component are shown in Figure 2.

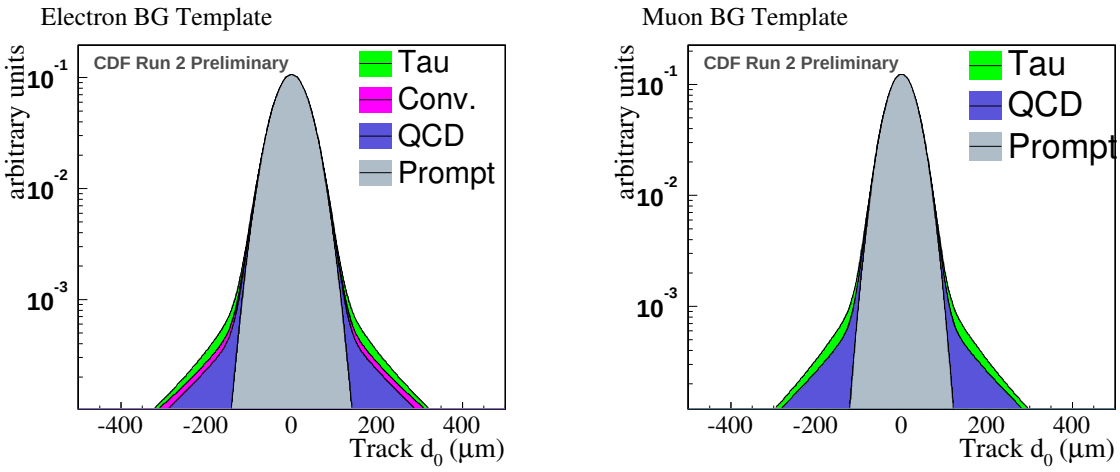

FIG. 2: Contributions to the background impact parameter distributions for electrons (left) and muons (right).

V. SYSTEMATIC UNCERTAINTIES

We consider two categories of systematic uncertainty: those affecting the background composition and d_0 shape, and those affecting the signal d_0 distribution. The background cross sections, efficiencies, and Monte Carlo modeling of acceptances, the tagging probability for jets in $W^{\pm}/Z^0$ and QCD events, and the sideband samples used to determine QCD backgrounds contribute to the first category of systematic uncertainty. Also affecting the background template are the uncertainties from fitting each background d_0 shape, from the extrapolation of the fraction of displaced QCD tracks from the low $\not\!\!E_T$ sideband, and from the potentially biased d_0 shape in the sample of identified conversions. Systematic effects of the first type are listed in Table II.

The second category of systematic error includes uncertainties affecting the kinematics of top decay which determine the observed track d_0 for a given proper t lifetime. Uncertainties in the parton distribution functions, the level of initial and final state radiation, and the calorimeter system's jet energy response are determined by varying these parameters in the Monte Carlo simulation. We also include the uncertainty in the detector resolution, which affects both the signal and background modeling, in this category. The effects of these variations on the top lifetime fit result are listed in Table III.

Systematic source	$\Delta N_{\text{electrons}}$	ΔN_{muons}
EWK/QCD estimate (stat)	1.1	0.8
MC Statistics	0.1	0.1
Cross sections	0.1	0.1
Trigger, ID scale factors	0.3	0.2
b-tagging scale factor	0.3	0.2
$W^{\pm}$ tag rate	3.6	2.7
QCD tag rate	0.9	0.7
QCD sidebands	0.6	0.4

	Var. in e bkgd. (RMS)	Var. in μ bkgd. (RMS)
Fit/statistics	7.8 μm	9.0 μm
QCD HF fraction	1.0 μm	0.8 μm
Conversion selection bias	0 μm	–

TABLE II: Systematic errors affecting the number of background events (top) and the shape of the background d_0 distribution (bottom).

Systematic source	Avg. variation in mean $c\tau_{fit}$
prompt resolution	18.5 μm
p.d.f.s	3.5 μm
ISR	0.5 μm
FSR	1.0 μm
Jet energy scale	0.3 μm

TABLE III: Systematic errors affecting the signal template distributions.

VI. RESULTS

We calculate the combined likelihood of the electron and muon data with respect to the templates created for $0 \leq c\tau_t \leq 500\mu$m. The maximum likelihood is attained with the 0 μm template; the fit result is shown in Figure 3.

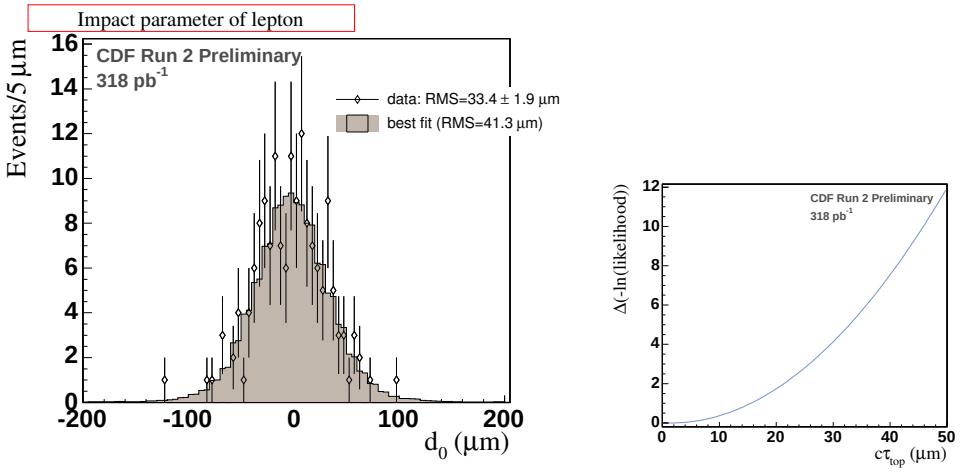

FIG. 3: Comparison of the lepton data to the expected distribution for $c\tau_t = 0$ μm (left), and the change in the negative log likelihood as a function of $c\tau_t$ (right).

We interpret this result using the Feldman-Cousins construction of confidence intervals [5], mapping the probability distribution function $P(c\tau_{\text{fit}}|c\tau_{\text{true}})$ using pseudo-experiments. We generate ensembles of simulated data corresponding to top lifetimes in the range $0\mu\text{m} \leq c\tau_{\text{gen}} \leq 100\mu\text{m}$. The systematic uncertainties described in Section V are incorporated into the pseudo-experiments: those uncertain quantities affecting the background d_0 shape are allowed

to vary within their total uncertainty in the pseudo-experiment trials. The systematic errors affecting the signal model are included by smearing the probability distributions for $c\tau_{\rm fit}$ before performing the likelihood-ratio ordering and extracting the confidence intervals. The confidence bands resulting from this procedure are displayed in Figure 4. Our observation $c\tau_{\rm fit} = 0$ μm thus corresponds to a limit of $c\tau_t < 52.5$ at 95% C.L.

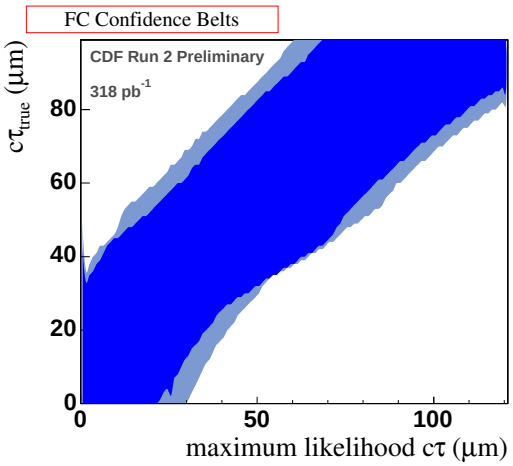

FIG. 4: Feldman-Cousins confidence intervals for the true top lifetime, as a function of the fit result $c\tau_{\rm fit}$.

Acknowledgments

We thank the Fermilab staff and the technical staffs of the participating institutions for their vital contributions. This work was supported by the U.S. Department of Energy and National Science Foundation; the Italian Istituto Nazionale di Fisica Nucleare; the Ministry of Education, Culture, Sports, Science and Technology of Japan; the Natural Sciences and Engineering Research Council of Canada; the National Science Council of the Republic of China; the Swiss National Science Foundation; the A.P. Sloan Foundation; the Bundesministerium fuer Bildung und Forschung, Germany; the Korean Science and Engineering Foundation and the Korean Research Foundation; the Particle Physics and Astronomy Research Council and the Royal Society, UK; the Russian Foundation for Basic Research; the Comision Interministerial de Ciencia y Tecnologia, Spain; and in part by the European Community's Human Potential Programme under contract HPRN-CT-20002, Probe for New Physics.

[1] S. Eidelman et al., Physics Letters B592, 1 (2004).
[2] F. Abe, et al., Nucl. Instrum. Methods Phys. Res. A **271**, 387 (1988); D. Amidei, et al., Nucl. Instum. Methods Phys. Res. A **350**, 73 (1994); F. Abe, et al., Phys. Rev. D **52**, 4784 (1995); P. Azzi, et al., Nucl. Instrum. Methods Phys. Res. A **360**, 137 (1995); The CDFII Detector Technical Design Report, Fermilab-Pub-96/390-E
[3] T. Sjostrand et al., High-Energy-Physics Event Generation with PYTHIA 6.1, Comput. Phys. Commun. **135**, 238 (2001).
[4] G. Corcella et al., HERWIG 6: An Event Generator for Hadron Emission Reactions with Interfering Gluons (including supersymmetric processes), JHEP **01**, 10 (2001).
[5] G. J. Feldman and R. D. Cousins, Phys. Rev. D **57**, 3873 (1998).